

Ultra-large actively tunable photonic band gaps via plasmon-analog of index enhancement

Emre Yüce,^{1,2} Zafer Artvin,^{3,4,5} Ramazan Sahin,⁶ Alpan Bek,^{1,2} and Mehmet Emre Tasgin^{3,*}

¹*Department of Physics, Middle East Technical University, 06800 Ankara, Turkey*

²*Center for Solar Energy Research and Applications (GÜNAM),*

Middle East Technical University, Dumlupınar Blvd. 1, 06800 Ankara, Turkey

³*Institute of Nuclear Sciences, Hacettepe University, 06800 Ankara, Turkey*

⁴*Department of Nanotechnology and Nanomedicine, Hacettepe University, Ankara, Turkey*

⁵*Central Laboratory, Middle East Technical University, 06800 Ankara, Turkey*

⁶*Faculty of Science, Department of Physics, Akdeniz University, 07058 Antalya, Turkey*

(Dated: December 22, 2024)

We present a novel method for active continuous-tuning of a band gap which has the great potential to revolutionize current photonic technologies. We study a periodic structure of x and y-aligned nanorod dimers. Refractive index of an y-polarized probe pulse can be continuously-tuned by the intensity of an x-polarized auxiliary (pump) pulse. Order of magnitude index-tuning can be achieved with a *vanishing loss* using the plasmon-analog of refractive index enhancement [PRB 100, 075427 (2019)]. Thus, a large band gap can be created from a non-existing gap via the auxiliary pulse. The new method, working for any crystal dimensions, can also be utilized as a *linear* photonic switch operating at tens of femtoseconds.

Ability of crafting materials at dimensions comparable to wavelength of light not only allowed control of electromagnetic radiation at nanoscale, but also made development of metamaterials [1], such as photonic crystals (PCs) [2–4], possible. PCs, periodically altering refractive index materials, reshape the propagation (dispersion) of the incident light and even can forbid it at certain propagation directions within some frequency ranges, named as photonic band gaps (PBGs) [5]. PBGs, whose structure depends on the periodicity and index contrast, can be utilized as waveguides [6], optical cavities [7], optical memories [8] and switches [9, 10]. This way PBGs enable on-chip photonic signal processing [11]. These structures can even enable control over quantum phenomena [12–14] such as spontaneous emission [15, 16] and entanglement [17] at nanoscale.

A conventional PC —whose PBG structure remains fixed after manufacturing— cannot operate, e.g., as a switch, although it is useful for photonic waveguide and cavity applications. External control of the constituent material’s refractive index, however, demonstrated to tune the PBG width about a few percent which allows the utilization of PCs as photonic switches. Refractive index of semiconductors (materials commonly employed in current PC technologies owing to their relatively-high index, $n=3.5-4$, and small absorption) can be tuned externally (actively) via optical heating [18], free-carrier excitation [19] and electronic Kerr-effect [10, 20]. While technique of free-carrier excitation provides the largest index change ($\sim 3\%$), its response time (tens of picoseconds) is much longer compared to the modulation time of the Kerr effect (a few femtosecond). Using the Kerr effect, in contrast, achievable index change is only $\sim 1\%$.

Metal nanostructures, which can localize the incident light into nm-sized hotspots, are also utilized for photonic technologies. Hybrid metastructures, created with semiconductors and metallic nanostructures, increase the versatility integrated photonic structures [21–23]. Yet, regarding the modulation depth, response time and metal-induced losses their functionalities are limited [21–23].

Therefore, a mechanism providing; (i) a large refractive index change (ii) minimal loss, (iii) short response time, and (iv) a large modulation depth will revolutionize the dynamic control of light on-a-chip. Faithfully, in this paper, we propose the utilization of a recently-discovered extraordinary index enhancement (control) scheme for achieving a game-changing control over the PBGs of a PC.

While plasmon analogs of electromagnetically induced transparency (EIT) [24–26], in the linear (called as Fano resonances [27–29]) and nonlinear response [30–33] have been demonstrated before; demonstration of the plasmon analog of index enhancement [34] could be achieved just recently [35]. Lavrinenko and colleagues [35] demonstrate that polarization response of a y-aligned silver nanorod to a y-polarized probe pulse can be controlled by the presence of an x-polarized auxiliary pulse, see Fig. 1. Owing to the shape resonance (selective coupling [36]) of nanorods; x,y-polarized pulse can excite “only” the x,y-aligned nanorods, respectively. Beyond studying the enhancement using a basic analytical model, which has widely been demonstrated to work very well for plasmonic path interference effects [32, 37, 38], Lavrinenko and colleagues also demonstrated the phenomenon via exact solutions of 3D Maxwell equations. This scheme not only enhances the refractive index more than 2-orders of magnitude, but also results a canceled absorption at the enhancement frequency —just as the same in its EIT counterpart [39]. This phenomenon allows us to adjust the “loss-free” refractive index of metamaterials without

* Correspondence: metasgin@hacettepe.edu.tr

sacrificing the probe signal to metallic losses.

In this paper, we show that plasmonic index enhancement is the dream-spouse for a photonic crystal. While other methods [10, 18–20] can tune the band gap size only about 2–3%, the presented scheme can *create* a large (e.g. 0.3 and 0.56 eV in Fig. 3) from a nonexistent gap only with a 6% filling ratio¹. One can achieve “any particular value” of the band gap width between 0–0.3 eV for any y-polarized probe pulse (E_1) by merely arranging the *intensity* ($\sim |E_2|^2$) of the x-polarized auxiliary (pump) pulse between $E_2=0-10E_1$, working in the low intensity regime. $|E_1|^2$ is the intensity of the weak probe field. Moreover, response time is limited within the plasmon lifetime (\sim fs [40]) and relation time (referred as $1/g$) since the scheme utilizes metal nanoparticles. In the case of silver nanorods, Ref. [35] originally studies, a 100 fs linear photonic switching can be achieved using 30 fs auxiliary pulse, see Fig. 5, where silver’s plasmon lifetime we use is already 40 fs long. It is apparent that using a small plasmon lifetime material, such as platinum [40, 41], should result much faster switching times².

Taking also the advantage of lossless medium, modulation depths of 110 dB (10^{11}) can be achieved using only 5 layers of silver dimers, one dimer in the $10 \times 100 \times 100$ volume of each index-enhanced region. This is because, supreme index enhancement can be achieved. The sample setup, plotted in Fig. 1, presents a 750 nm long enhanced photonic crystal on a PC-waveguide chip employing CMOS-compatible noble metal (silver) materials.

Though we content this prominent work with propagation through a single direction³, since we do not aim an exact simulation of an already conducted experiment, the method is applicable to crystal dimension obviously. (See also the discussion in the following text.) Index enhancement scheme, appearing via the coupling of the two orthogonal nanorods, can be obtained also on easier-to-manufacture structures.

Utilizing index-enhanced materials for periodic structures, actually, is not a new idea [42, 43], employed cold atom systems. Implementation of the plasmon analog of the phenomenon, however, provides a feasible “loss-free” backbone for PC technologies. Plasmon index enhancement has been exploited in Ref. [44] for achieving a continuously-tunable Cherenkov-radiation-based particle detector, ignoring the periodicity effects.

Index-enhancement scheme.— Fig. 1 demonstrates a sample setup for implementing index-enhancement

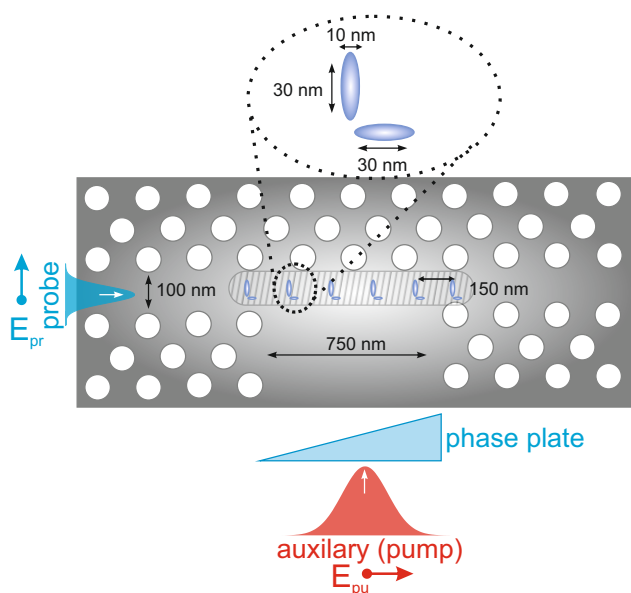


FIG. 1. A sample setup for the continuous band gap tuning (Fig. 4) and femtosecond photonic switch (Fig. 5). Probe ($E_1\hat{y}$) and auxiliary ($E_2\hat{x}$) pulses reach the periodic layers of nanorod dimers via defect waveguides. Intensity and phase of auxiliary pulse controls the presence and width of the photonic bad gap (Fig. 4). The phase plate matches the phase-difference between the aux and probe pulses at all dimers. When an ultrashort auxiliary pulse is employed the same periodic structure behaves as a linear photonic switch (Fig. 5).

phenomenon for on-chip photonic operations. 5 layers of silver nanorod dimers (see the inset) switches the transmission of a y-polarized probe pulse (E_1) of frequency ω via an x-polarized auxiliary (pump) pulse (E_2). When the auxiliary pulse is off, the refractive index of $V_{\text{rod}}=10 \times 10 \times 30$ sized nanorods becomes exceedingly small for a density of 1 dimer in volume $V_{\text{site}}=150 \times 100 \times 100 \text{ nm}^3$. Here 150 nm is the periodicity and 100 nm corresponds to width and depth of the cavity in which silver dimers are placed. Filling ratio of the index-enhanced layer, a single dimer in each one, is $10/150 \simeq 6\%$. Thus, probe is transmitted with a relatively small absorption, i.e., 35%. (Probe can be transmitted also without any absorption, see below.) When the auxiliary pulse is turned on, with amplitudes $E_2 = 10E_1$ and $100E_1$, however, effective refractive index of the thin layers (10 nm length) is enhanced dramatically, see Fig. 2a, thus turning ON a PBG of width ~ 0.3 eV and ~ 0.56 eV, respectively. See Fig 3a. The x-polarized auxiliary pulse couples only to the x-aligned silver nanorod and x-aligned nanorod affects the response of the y-aligned nanorod via a coupling through the hotspot appearing at the intersection of the two orthogonal rods. When the auxiliary pulse is present, y-polarized nanorod gives different polarization responses ($\chi_1 = P_1/E_1$) for different values of the probe field E_1 .

¹ Filling ratio of a silver dimer in Fig. 1 is 0.1%.

² Using a material of larger damping also necessitates a larger coupling strength g between the two nanorods, thus a smaller relaxation time, for the enhancement scheme to be observable.

³ Structure need not be one-dimensional. We only consider a single propagation direction by calculating an average polarization density on the other periodicity directions, if exist. In Fig. 1, there are only 5 layer nanodimers and no periodicity assumed in other directions.

Dynamics of such a coupled system can be described by a basic model [35, 44]

$$\ddot{x}_1 + \gamma_1 \dot{x}_1 + \omega_1^2 x_1 - gx_2 = \tilde{E}_1(t), \quad (1)$$

$$\ddot{x}_2 + \gamma_2 \dot{x}_2 + \omega_2^2 x_2 - gx_1 = \tilde{E}_2(t), \quad (2)$$

which is very successful in demonstrating the Fano-like path-interference effects in plasmonic nanostructures [32, 37, 38]. FDTD simulations in Ref. [35], also demonstrate the phenomenon. $\gamma_1 = \gamma_2 = 0.026\omega_0^2$, $\omega_1 = \omega_2 = \omega_0$ and $g = 0.06\omega_0$ [35] are the damping rates, resonances and the coupling between the two plasmon oscillations of the two nanorod, respectively. ω_0 is the resonance of both nanorods. Here, only $\gamma_{1,2}$ is different from the one of Ref. [35] since we determine the damping rates of nanorods from experimental dielectric function of silver. Actually, such a tidy choice of parameters is not necessary for this initial work which aims to present the implementation of the phenomenon for photonic technologies.

For a monochromatic auxiliary pulse $E_2 \sim e^{-i\omega t}$, of the same frequency with the probe, the exact solution for the susceptibility of the medium

$$\chi(\omega) = f\omega_0^2 \frac{\delta_2 + ge^{-i\phi} E_2/E_1}{\delta_1 \delta_2 - g^2} \quad (3)$$

can be obtained [35, 44]. The dimensionless oscillator strength f is determined by setting nonenhanced susceptibility $\chi(\omega = \omega_0, g = 0) = f/(\gamma_1/\omega_0)$ [44] to P_1/E_1 , with P_1 is the polarization density calculated for ellipsoid nanorods [35, 44, 45], for 1 dimer in index-enhanced layer (10 nm), with volume $V_{\text{layer}}=10 \times 100 \times 100 \text{ nm}^3$ in Fig. 1.

Since the auxiliary field, in our case an ultrashort pulse, has a broad frequency band, we take $\tilde{E}_2 = \sum_{\omega} E_2 e^{-i\phi} \exp[-(\omega - \Omega)^2/(\Delta\omega)^2] e^{-i\omega t}$ pulse unlike Ref. [35]. We solve Eqs. (1-2) in the frequency domain for the Gaussian auxiliary pulse. Fig. 2 plots the real and imaginary parts of the enhanced index⁴ for $E_2 = 100E_1$, $10E_1$ and 0. We note that a double resonance for $E_2 = 0$ appears, because coupling between the two nanorods exists when the auxiliary pulse is turned off.

In Fig. 2b, we observe that imaginary part of the index becomes zero almost at the same frequency (vertical dashed-line) for $E_2 = 100E_1$ and $10E_1$, where the index becomes superiorly enhanced.

The phase plate.— Setup in Fig. 1 includes a critical apparatus; a phase plate. Eq. (3) shows that the phase-difference between the auxiliary and probe pulse, $e^{-i\phi}$, plays an important role for the index enhancement to appear. The aux-probe phase-differences for the first

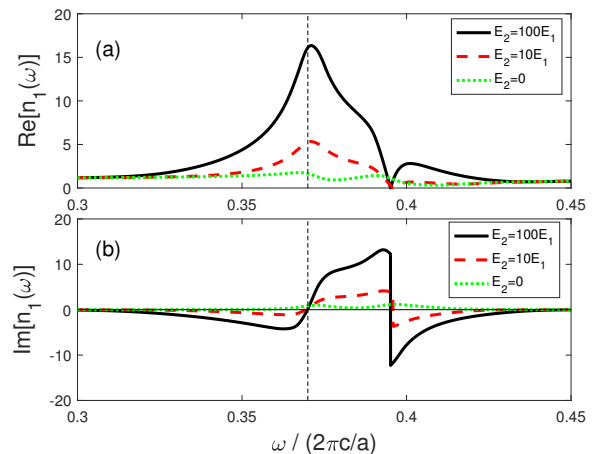


FIG. 2. (a) Real and (b) imaginary parts of the refractive index. Index of the y-polarized probe pulse is controlled by the intensity of the auxiliary pulse (E_2). Index is both enhanced and real at $\omega_{\text{enh}}=0.37 \times 2\pi c/a$. ($a=150 \text{ nm}$) Without the periodicity, probe pulse is amplified, e.g., to the left of ω_{enh} .

and second dimer are not the same, since the probe does not have the same phase at different dimers (x-positions). Hence, when the first dimer is set to enhanced index (for y-polarized probe), the second dimer can possess a non-enhanced index; destroying the periodicity. Thus, we rephase the front of the auxiliary pulse with a phase plate either in the entrance of the aux port of the waveguide, or in front of (or inside) the auxiliary source. **Such a necessity for phase-tuning, most probably, is the reason large PBG changes cannot be observed in experiments with periodic nanoparticles [21–23].**

Photonic bands.— In Fig. 3a, we present the transmission and reflection for the 5-layer index-enhanced PC of dimers of periodicity $a=150 \text{ nm}$ and filling ratio of $10/150 \sim 6\%$. It is striking that: while there exists a large amount of gain in the left of $\omega_{\text{enh}} \simeq 0.37 \times 2\pi c/a$ in Fig. 2b, Fig. 3a shows that PBG, the 5-layer enhanced PC creates, can turn-OFF the transmission in a wide frequency region both for $E_2 = 100E_1$ and $10E_1$. We note that, in the figures we scale the frequencies by $\omega_a = 2\pi c/a$ and momentum-vector by $k_a = 2\pi/a$ with $a=150 \text{ nm}$. In determining the natural band gap region, we first calculate the band diagram for the constant index $n = n(\omega_{\text{enh}})$, then we choose periodicity a accordingly as performed in Ref. [42].

We also calculate the photonic band structure in Fig. 4, which appears quite similar to the one for index enhancement in multilevel atomic ensembles []. The modulation depth for the $5 \times 150 = 750 \text{ nm}$ enhanced PC, at $\omega_{\text{enh}} \simeq 0.37$ calculated by transfer matrix method [47] (Fig. 3) and via band structure damping ($e^{ik_I a}$)⁵, are similar, where k_I is the imaginary part of the wavevector in Fig. 4 at ω_{enh} . Since the enhanced PC dimensions are quite small, modulation depth can be

⁴ We note that sign of the index is determined by choosing the real part of index positive, similar to performed in EIT counter-part of the index enhancement [46].

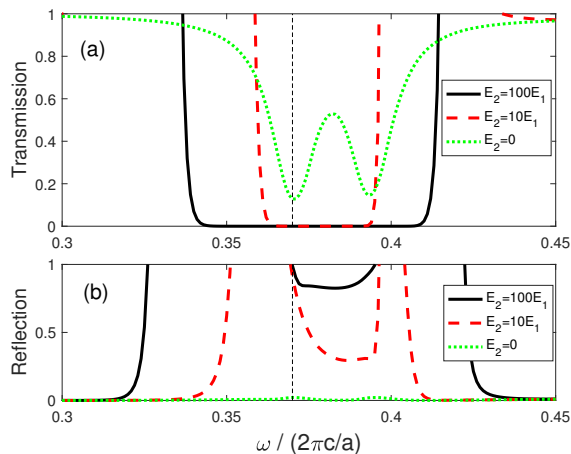


FIG. 3. (a) Transmission and (b) reflection from only 5 layers of silver nanorods crystal (Fig. 1). $E_2 = 100E_1$ and $10E_1$ display photonic band gaps even in the left of $\omega_{\text{enh}}=0.37$ (vertical line) where there is a strong gain (Fig. 2b). The width and existence of the band gap can be continuously-tuned by the auxiliary pulse intensity.

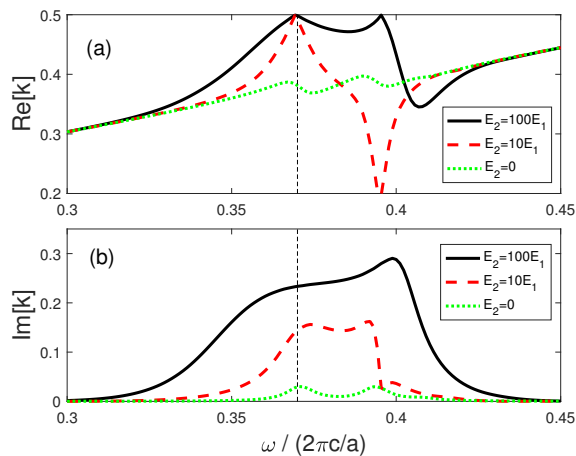


FIG. 4. Photonic band diagrams for a periodic structure of silver nanorod dimers (Fig. 1) with a filling ratio of 6.2%. For $\omega = \omega_{\text{enh}}=0.37$ (vertical line), index is real (Fig. 2b) and $E_2 = 100E_1$ and $10E_1$ display a band gap. Band diagrams are similar to the one obtained for index enhancement in atomic ensembles [26, 42].

increased by setting more layers into the enhanced PC.

PC operation regimes.— There can be several options for the operation regions in utilizing the system as a photonic switch. (a) PC can be operated at $\omega = \omega_{\text{enh}}$, but transmission in the switch on mode drops to 0.15 for this regime, see Fig. 3a. (b) One can choose a better switch-on transmission 0.55 for $\omega \simeq 0.38$, since absorption in the switch-off mode is not important for this application. (c) Index-enhancement scheme is an active medium. It displays a substantial gain, e.g., between $\omega=0.35$ - 0.37 , when the auxiliary (pump) field is set to $E_2 = 10E_1$. Thus,

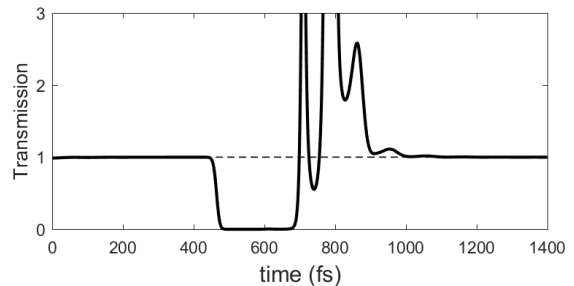


FIG. 5. When the applied auxiliary field E_2 is an ultrashort pulse ($\Delta t=30$ fs), the crystal of silver dimers behaves as a linear photonic switch. The transmission (switch) along the x-direction is shutdown when the auxiliary pulse is on the y-aligned nanorods in Fig. 1. The switch remains off for $\simeq 200$ fs. Length of this interval, limited by the damping of the silver rod ($\tau \sim 38$ fs), can be refined (shortened) substantially using a bad-quality nanostructure. For instance it is 1.3 fs in platinum [41].

working, for instance, $\omega = 0.36$ enhances the transmitted pulse several orders of magnitude for $E_2 = 10E_1$ via gain, but, suppresses the transmission when auxiliary is turned to $E_2 = 100E_1$ due to the band gap. Thus, the modulation depth between switch-on (former case) and switch-off (latter case) can be increased further, actually, leading to unimaginable values. While we demonstrate the switch mechanism for quite different values of the auxiliary field, i.e., $E_2 = 100E_1$ and $10E_1$, an optimization can be carried out for smaller differences.

Response time.— In Fig. 5, we present the time development of the transmitted pulse when a 30 fs, auxiliary pulse passes through the enhanced PC. We observe that, although the temporal width of the auxiliary pulse is 30 fs PBG remains off for about ~ 200 fs. This limitation, actually, occurs due to two transient times. The decay time of the surface plasmon oscillations on silver, used in this work [35, 44], is already about 40 fs. The switch time is also determined by the relaxation time, appearing due to the interaction between the two nanorods⁵. After $t \simeq 700$ fs, we observe the gain amplification of the transmission (it reaches ...) during the PNG off regime. This transient also lasts ~ 200 fs, but, increases the modulation depth between $t = 600$ fs and 700 fs dramatically. When, for instance, platinum nanorods, of decay time ~ 1 fs are used in the enhanced PC, much faster response times can be achieved. We remark that, a larger damping rate necessitates also a larger coupling g for enhancement scheme to appear.

Periodicity on 2D and 3D.— Index enhancement scheme depends critically on the phase difference between the probe and the auxiliary pulses. When there is periodicity of nanodimers along the z-axis in Fig. 1, there would

⁵ In a coupled system, transient time is determined by the minimum of the damping rates.

appear no problem. Because, the phase of the auxiliary pulse is constant in the x-z plane. On working the periodicity along the propagation direction of the auxiliary pulse, y, however, one needs to take care of the different positions (so phases) of adjacent dimer arrays along the y-direction. Traveling along the y-directions, the first and the second dimer arrays show different phase-differences for the auxiliary and probe pulses. Index enhancement scheme can be different, even be demolished, in this case. This problem, however, can be circumvented in two ways. (i) One can choose the y-periodicity of the PC such that at a desired operation wavelength altering phases, $e^{i\phi_1}$ and $e^{i\phi_2}$, overlap. (ii) A second approach: once could induce an appropriate phase dilation also in the probe field along the y-axis either in the waveguide input or just before PC input. One important point to stress is: in the enhancement scheme, index can be superiorly strengthened such that a single dimer array becomes sufficient for switching operations.

In summary, we show that recently-explored index en-

hancement for plasmonic nanoparticles [35] can be utilized in photonic crystal technologies for achieving far-off-records photonic band gap tuning and modulation depths. This is because, available adjustment of refractive index, using this scheme, is incomparably larger than the currently applied methods [10, 18–20]. Index enhancement, achieved with a “vanishing loss”, is such a large value (as in its EIT-counterpart [42, 43, 46]) that using very small filling ratio for nanoparticles becomes sufficient. Switching time of the PBG is determined by the decay rate of the metal nanoparticles, so, it is in the femtosecond regime. Vanishing loss at the enhancement frequency can be utilized as undamped, but can be turned on and off, cavities at specific frequencies important for quantum optics (information) applications [48–51].

Therefore, implementation of the plasmon-analog of refractive index enhancement (control) to photonic crystals provides a revolutionary instrument for photonic applications.

-
- [1] Yongmin Liu and Xiang Zhang, “Metamaterials: a new frontier of science and technology,” *Chemical Society Reviews* **40**, 2494–2507 (2011).
- [2] Eli Yablonovitch, “Inhibited spontaneous emission in solid-state physics and electronics,” *Physical Review Letters* **58**, 2059 (1987).
- [3] Eli Yablonovitch, TJ Gmitter, and Kok-Ming Leung, “Photonic band structure: The face-centered-cubic case employing nonspherical atoms,” *Physical Review Letters* **67**, 2295 (1991).
- [4] J. E. G. J. Wijnhoven and W. L. Vos, “Preparation of photonic crystals made of air spheres in titania,” *Science* **281**, 802–804 (1998).
- [5] M. D. Leistikow, A. P. Mosk, E. Yeganegi, S. R. Huisman, A. Lagendijk, and W. L. Vos, “Inhibited spontaneous emission of quantum dots observed in a 3D photonic band gap,” *Phys. Rev. Lett.* **107**, 193903–1–5 (2011).
- [6] JC Knight, TA Birks, P St J Russell, and DM Atkin, “All-silica single-mode optical fiber with photonic crystal cladding,” *Optics Letters* **21**, 1547–1549 (1996).
- [7] Yoshihiro Akahane, Takashi Asano, Bong-Shik Song, and Susumu Noda, “High-q photonic nanocavity in a two-dimensional photonic crystal,” *Nature* **425**, 944–947 (2003).
- [8] Eiichi Kuramochi, Kengo Nozaki, Akihiko Shinya, Koji Takeda, Tomonari Sato, Shinji Matsuo, Hideaki Taniyama, Hisashi Sumikura, and Masaya Notomi, “Large-scale integration of wavelength-addressable all-optical memories on a photonic crystal chip,” *Nature Photon.* **8**, 474–481 (2014).
- [9] Tijmen G Euser, Hong Wei, Jeroen Kalkman, Yoonho Jun, Albert Polman, David J Norris, and Willem L Vos, “Ultrafast optical switching of three-dimensional inverse opal photonic band gap crystals,” *Journal of Applied Physics* **102**, 053111 (2007).
- [10] Emre Yüce, Georgios Ctistis, Julien Claudon, Emmanuel Dupuy, Robin D Buijs, Bob de Ronde, Allard P Mosk, Jean-Michel Gérard, and Willem L Vos, “All-optical switching of a microcavity repeated at terahertz rates,” *Optics Letters* **38**, 374–376 (2013).
- [11] Jian Wang and Yun Long, “On-chip silicon photonic signaling and processing: a review,” *Science Bulletin* **63**, 1267–1310 (2018).
- [12] Serge Haroche and Daniel Kleppner, “Cavity quantum electrodynamics,” *Phys. Today* **42**, 24–30 (1989).
- [13] Peter Lodahl, A Floris Van Driel, Ivan S Nikolaev, Arie Irman, Karin Overgaag, Daniël Vanmaekelbergh, and Willem L Vos, “Controlling the dynamics of spontaneous emission from quantum dots by photonic crystals,” *Nature* **430**, 654–657 (2004).
- [14] Kristian Høeg Madsen, Serkan Ates, Toke Lund-Hansen, A Löffler, S Reitzenstein, A Forchel, and Peter Lodahl, “Observation of non-markovian dynamics of a single quantum dot in a micropillar cavity,” *Physical Review Letters* **106**, 233601 (2011).
- [15] Marlan O Scully, “Single photon subradiance: quantum control of spontaneous emission and ultrafast readout,” *Physical Review Letters* **115**, 243602 (2015).
- [16] Marlan O Scully and Anatoly A Svidzinsky, “The super of superradiance,” *Science* **325**, 1510–1511 (2009).
- [17] Mehmet Emre Tasgin, “Many-particle entanglement criterion for superradiantlike states,” *Physical Review Letters* **119**, 033601 (2017).
- [18] Graham T Reed and Andrew P Knights, *Silicon photonics: an introduction* (John Wiley & Sons, 2004).
- [19] Vilson R Almeida, Carlos A Barrios, Roberto R Panepucci, and Michal Lipson, “All-optical control of light on a silicon chip,” *Nature* **431**, 1081–1084 (2004).
- [20] Georgios Ctistis, Emre Yuce, Alex Hartsuiker, Julien Claudon, Maela Bazin, Jean-Michel Gérard, and Willem L Vos, “Ultimate fast optical switching of a planar microcavity in the telecom wavelength range,” *Applied Physics Letters* **98**, 161114 (2011).
- [21] Kebin Fan and Willie J Padilla, “Dynamic electromag-

- netic metamaterials,” *Materials Today* **18**, 39–50 (2015).
- [22] Qiong He, Shulin Sun, Lei Zhou, *et al.*, “Tunable/reconfigurable metasurfaces: Physics and applications,” *Research* **2019**, 1849272 (2019).
- [23] Lei Kang, Ronald P Jenkins, and Douglas H Werner, “Recent progress in active optical metasurfaces,” *Advanced Optical Materials* **7**, 1801813 (2019).
- [24] MD Lukin and Ataç Imamoglu, “Controlling photons using electromagnetically induced transparency,” *Nature* **413**, 273–276 (2001).
- [25] K-J Boller, A Imamoglu, and Stephen E Harris, “Observation of electromagnetically induced transparency,” *Physical Review Letters* **66**, 2593 (1991).
- [26] M. O. Scully and M. S. Zubairy, *Quantum Optics* (Cambridge University Press, New York, 1997).
- [27] Boris Luk’yanchuk, Nikolay I Zheludev, Stefan A Maier, Naomi J Halas, Peter Nordlander, Harald Giessen, and Chong Tow Chong, “The fano resonance in plasmonic nanostructures and metamaterials,” *Nature materials* **9**, 707 (2010).
- [28] Mikhail F Limonov, Mikhail V Rybin, Alexander N Podubny, and Yuri S Kivshar, “Fano resonances in photonics,” *Nature Photonics* **11**, 543 (2017).
- [29] Bo Peng, Şahin Kaya Özdemir, Weijian Chen, Franco Nori, and Lan Yang, “What is and what is not electromagnetically induced transparency in whispering-gallery microcavities,” *Nature communications* **5**, 5082 (2014).
- [30] Jérémy Butet and Olivier JF Martin, “Fano resonances in the nonlinear optical response of coupled plasmonic nanostructures,” *Optics Express* **22**, 29693–29707 (2014).
- [31] Shailendra K Singh, M Kurtulus Abak, and Mehmet Emre Tasgin, “Enhancement of four-wave mixing via interference of multiple plasmonic conversion paths,” *Physical Review B* **93**, 035410 (2016).
- [32] Mehmet Emre Tasgin, Alpan Bek, and Selen Postaci, “Fano resonances in the linear and nonlinear plasmonic response,” in *Fano Resonances in Optics and Microwaves* (Springer, 2018) pp. 1–31.
- [33] Selen Postaci, Bilge Can Yildiz, Alpan Bek, and Mehmet Emre Tasgin, “Silent enhancement of sers signal without increasing hot spot intensities,” *Nanophotonics* **7**, 1687–1695 (2018).
- [34] Marlan O Scully, “Enhancement of the index of refraction via quantum coherence,” *Physical Review Letters* **67**, 1855 (1991).
- [35] Ali Panahpour, Abolfazl Mahmoodpoor, and Andrei V Lavrinenko, “Refraction enhancement in plasmonics by coherent control of plasmon resonances,” *Physical Review B* **100**, 075427 (2019).
- [36] David Andrews, Thomas Nann, and Robert H Lipson, *Comprehensive nanoscience and nanotechnology* (Academic Press, 2019).
- [37] Xiaohua Wu, Stephen K Gray, and Matthew Pelton, “Quantum-dot-induced transparency in a nanoscale plasmonic resonator,” *Optics express* **18**, 23633–23645 (2010).
- [38] Andrea Lovera, Benjamin Gallinet, Peter Nordlander, and Olivier JF Martin, “Mechanisms of fano resonances in coupled plasmonic systems,” *ACS Nano* **7**, 4527–4536 (2013).
- [39] Michael Fleischhauer, Atac Imamoglu, and Jonathan P Marangos, “Electromagnetically induced transparency: Optics in coherent media,” *Reviews of Modern Physics* **77**, 633 (2005).
- [40] Igor Zoric, Michael Zach, Bengt Kasemo, and Christoph Langhammer, “Gold, platinum, and aluminum nanodisk plasmons: material independence, subradiance, and damping mechanisms,” *ACS Nano* **5**, 2535–2546 (2011).
- [41] Bilge Can Yildiz, Alpan Bek, and Mehmet Emre Tasgin, “Plasmon lifetime enhancement in a bright-dark mode coupled system,” *Physical Review B* **101**, 035416 (2020).
- [42] Mehmet Emre Tasgin, Özgür Esat Müstecaphoğlu, and MÖ Oktel, “Photonic band gap in the triangular lattice of bose-einstein-condensate vortices,” *Physical Review A* **75**, 063627 (2007).
- [43] ÖE Müstecaphoğlu and MÖ Oktel, “Photonic band gap via quantum coherence in vortex lattices of bose-einstein condensates,” *Physical Review Letters* **94**, 220404 (2005).
- [44] Mehmet Günay, You-Lin Chuang, and Mehmet Emre Tasgin, “Tunable Cherenkov radiation-based detectors via plasmon index enhancement,” *Nanophotonics*: Ahead of publication Nanophotonics; <https://www.degruyter.com/view/journals/nanoph/ahead-of-print/article-10.1515-nanoph-2020-0081/article-10.1515-nanoph-2020-0081.xml> arXiv preprint arXiv:1911.08159 (2019).
- [45] Craig F Bohren and Donald R Huffman, *Absorption and scattering of light by small particles* (John Wiley & Sons, 2008).
- [46] Michael Fleischhauer, Christoph H Keitel, Marlan O Scully, Chang Su, BT Ulrich, and Shi-Yao Zhu, “Resonantly enhanced refractive index without absorption via atomic coherence,” *Physical Review A* **46**, 1468 (1992).
- [47] Zhi-Yuan Li, “Principles of the plane-wave transfer-matrix method for photonic crystals,” *Science and Technology of Advanced Materials* **6**, 837 (2005).
- [48] Andreas Reiserer and Gerhard Rempe, “Cavity-based quantum networks with single atoms and optical photons,” *Reviews of Modern Physics* **87**, 1379 (2015).
- [49] Marlan O Scully, M Suhail Zubairy, Girish S Agarwal, and Herbert Walther, “Extracting work from a single heat bath via vanishing quantum coherence,” *Science* **299**, 862–864 (2003).
- [50] Ali ÜC Hardal and Özgür E Müstecaphoğlu, “Superradiant quantum heat engine,” *Scientific Reports* **5**, 12953 (2015).
- [51] Yueyang Zou, Yue Jiang, Yefeng Mei, Xianxin Guo, and Shengwang Du, “Quantum heat engine using electromagnetically induced transparency,” *Physical Review Letters* **119**, 050602 (2017).